International Journal of Modern Physics C
Vol. 20, No. 8 (2009) 1145–1153

World Scientific
www.worldscientific.com

SIMULATION OF GAS FLOW IN MICROTUBES BY LATTICE BOLTZMANN METHOD

HAIBO HUANG* and XI-YUN LU
Department of Modern Mechanics
University of Science and Technology of China
Hefei 230026, China
**huanghb@ustc.edu.cn*

Received 6 January 2009
Accepted 31 March 2009

Isothermal gas flow in microtubes with a sudden expansion or contraction is studied numerically by lattice Boltzmann method. An axisymmetric D2Q9 model is used to simulate gas slip flow in micro-circular pipes. With the boundary condition combined specular and bounce-back schemes, the computed results are in excellent agreement with analytical solution for straight microtube. For the gas flow in the expanded or constricted tubes, we carried out simulations of several Knudsen numbers with inlet/outlet pressure ratio 3. It is found the pressure drop in each section can be predicted well by the theory of straight tubes. For smaller Knudsen number, flow separation in the expanded tube is observed. While for large Knudsen number, there is no vortex at corner and the streamlines are attached to boundary. In the constricted tube, the vortex at corner is very weak. These results are consistent with some experimental conclusions.

Keywords: Lattice Boltzmann; slip flow; microtube; microfluidics; Knudsen numbeer.

1. Introduction

MEMS (Micro-Electro-Mechanical-Systems) devices with dimensions ranging from 100 to 1 microns have found many applications in engineering and scientific researches.[1] MEMS are often operated in gaseous environments at standard conditions in which the dynamics associated with MEMS can exhibit rarefied phenomena and compressibility effects.[2] Usually the Knudsen number Kn is used to identify the effects. Kn is the ratio of the mean free path λ to the characteristic length D. Generally speaking, the continuum assumption for Navier–Stokes (NS) equations may break down if $Kn > 0.01$. For the flow case $0.01 < Kn < 0.1$, a slip velocity would appear in the wall boundary. The value of $0.1 < Kn < 10$ are associated with a transition flow regime.

The rarefied gas slip flow in microchannels or tubes have been investigated experimentally or analytically.[2,3] Numerical simulations can be carried out by solving NS equation[4] or the direct simulation Monte Carlo (DSMC) method.[5] Recently,

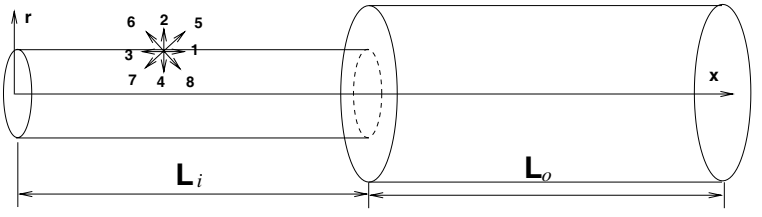

Fig. 1. Geometry of microtubes with a sudden expansion/contraction and D2Q9 model.

the lattice Boltzmann method (LBM) is based on meso-scale level and has been applied to simulate the microflows.[6–8,18,19] LBM is more computationally efficient comparing with the DSMC method because it is only dependent upon the number of mesh points and the lattice model.[6]

However, previous LBM study of microflow is only concentrated in microchannel. As we know, circular microtubes have been widely used in many MEMS devices, such as micropumps, microactuators, microheat exchangers, microsensors, biological cell reactors, and selective membranes.[3] Fluid flow in micropumps or microactuators is often through channels or tubes with contraction/expansion transitions, changes in cross-sectional area, bends or branching.[9]

In order to understand the flow physics or even improve relevant microdevices, here we focus on the flow in circular microtube with sudden expansion or contraction (Fig. 1). First, through inserting the source term into the microevaluation equation,[10] a revised axisymmetric D2Q9 LBM is used to simulate axisymmetric flows in microtube.[19] Then the model was validated by simulation of microflow in a straight circular tube and making comparison with analytical solutions.[9]

2. Numerical Methods

Among many different lattice Boltzmann equation (LBE) models, the lattice Bhatnagar–Gross–Krook (LBGK) model is the simplest one because it only has one scalar relaxation parameter. Here our axisymmetric LBM is derived from LBGK D2Q9 model.

We describe our model in pseudo-Cartesian coordinates (x, r), $f_i(x, r, t)$ is the distribution function for particles with velocity $\mathbf{e}_i$ at position (x, r) and time t. The basic discrete-velocity Boltzmann kinetic equation is

$$f_i(x + e_{ix}\delta_t, r + e_{ir}\delta_t, t + \delta_t) - f_i(x, r, t) = \frac{1}{\tau}[f_i^{\mathrm{eq}}(x, r, t) - f_i(x, r, t)] + h_i\,, \tag{1}$$

where τ is the collision relax time constant, and δ_x and δ_t are the lattice spacing and timestep size, respectively. $f_i^{\mathrm{eq}}(x, r, t)$ is the equilibrium distribution function

defined as[15]

$$f_i^{\mathrm{eq}}(x,r,t) = \omega_i \rho \left[1 + \frac{\mathbf{e}_i \cdot \mathbf{u}}{c_s^2} + \frac{(\mathbf{e}_i \cdot \mathbf{u})^2}{2c_s^4} - \frac{\mathbf{u}^2}{2c_s^2}\right] \quad i = 0, 1, 2, \ldots, 8\,,$$

where $c_s = c/\sqrt{3}$, $c = \delta_x/\delta_t$, $\omega_0 = 4/9$, $\omega_i = 1/9$ ($i = 1, 2, 3, 4$), $\omega_i = 1/36$ ($i = 5, 6, 7, 8$).

In our D2Q9 model, the nine discrete velocities of our model (refer to Fig. 1) are defined as following, $\mathbf{e}_0 = 0$, $\mathbf{e}_i = (\cos[(i-1)\pi/2], \sin[(i-1)\pi/2])c$, $i = 1, 2, 3, 4$ and $\mathbf{e}_i = \sqrt{2}(\cos[(i-5)\pi/2+\pi/4], \sin[(i-5)\pi/2+\pi/4])c$, $i = 5, 6, 7, 8$. The characteristic speed c can be related to the reference temperature by $c = \sqrt{3RT}$. The macroscopic density ρ and momentum $\rho\mathbf{u}$ are defined as $\rho = \sum_{i=0}^{8} f_i$, $\rho u_\alpha = \sum_{i=0}^{8} f_i e_{i\alpha}$, and $p = \rho c_s^2$. In Eq. (1), the "source" terms can be written as

$$h_i = \delta_t h_i^{(1)} + \delta_t^2 h_i^{(2)}\,, \tag{2}$$

where $h_i^{(1)}$ and $h_i^{(2)}$ are the terms added into the LBE, which can be calculated through below Eqs. (3) and (4), respectively.

$$h_i^{(1)} = -\frac{\omega_i \rho u_r}{r}\,, \tag{3}$$

$$\begin{aligned} h_i^{(2)} = {} & \frac{\omega_i}{2r}\left(\partial_r \frac{\rho}{3} + \partial_x \rho u_x u_r + \partial_r \rho u_r u_r\right) + \frac{3\omega_i \rho \nu}{r}(e_{ix}\partial_r u_x + e_{ir}\partial_r u_r) \\ & - \frac{3\omega_i \rho \nu}{r^2} u_r e_{ir} - 3\omega_i \rho \left(\frac{u_x u_r}{r} e_{ix} + \frac{u_r u_r}{r} e_{ir}\right) \\ & - (1-\tau)\omega_i \left(\frac{1}{r}\partial_x \rho u_r e_{ix} - \frac{\rho u_r}{r^2} e_{ir} + \frac{\partial_r \rho u_r}{r} e_{ir}\right)\,. \end{aligned} \tag{4}$$

Through the Chapman–Enskog Expansion as Refs. 10 and 12, the continuity equation and momentum equations in Ref. 3 for a compressible fluid in the pseudo-Cartesian coordinates (x, r) can be recovered from our axisymmetric D2Q9 model.[19]

Comparing with our model, the model of Halliday *et al.*[10] missed some terms. That would lead to a large error for simulating the flows in constricted pipes. The present model is found more accurate and stable than previous models.[12–14] The detailed comparisons between different axisymmetric models[13,14] can be found in Ref. 12. For the velocity derivatives in Eq. (4), most velocity gradient terms can be obtained from high-order momentum of distribution function, which is consistent with the philosophy of the LBM.[11]

In the above equations, the relax time constant τ and the fluid kinetic viscosity ν satisfies equation $\nu = c_s^2(\tau - 0.5\delta_t)$. To simulate the microflow, the parameter τ and Kn are correlated as,[7] $\tau/\delta_t = KnN_D/\sqrt{\pi/6} + 0.5$, where N_D is the lattice number in the tube diameter, Kn is local Knudsen number. The local Kn can be calculated by $Kn = Kn_o p_o/p(x, r)$, where Kn_o and p_o are the Kn and the pressure at the outlet.

For wall boundary condition, bounce-back scheme is usually used to realize nonslip boundary condition when simulation continuum flow. On the other hand,

specular reflection scheme[6] can be applied to free-slip boundary condition where no momentum is to be exchanged with the wall along the tangential component. For real gas flow in microtubes, a combination of the two schemes is considered here. To describe boundary condition treatment, a wall $\partial\Omega$ is completely specified. For a point $\mathbf{x}(\mathbf{x} \in \partial\Omega)$, $\mathbf{n}$ is the inward unit normal vector of the wall. After streaming step is implemented, the unknown distribution functions of $f_i(\mathbf{x}, t)$, $\mathbf{e}_i \cdot \mathbf{n} > 0$ (i.e. f_4, f_7, f_8 in up wall of tube in Fig. 1) can be evaluated by[7,16]

$$f_i(\mathbf{x}, t) = bf_j(\mathbf{x}, t) + (1 - b)f_k(\mathbf{x}, t)\,, \tag{5}$$

where $f_j(\mathbf{x}, t)$ is the distribution function in $\mathbf{e}_j$ direction, where $\mathbf{e}_i - \mathbf{e}_j = 2\mathbf{e}_i$, and $f_k(\mathbf{x}, t)$ is the distribution function in $\mathbf{e}_k$ direction, where $\mathbf{e}_i - \mathbf{e}_k = 2\mathbf{n}$. b is the bounce-back probability chosen 0.7 as Ref. 7.

For the inlet/outlet boundary conditions, the pressure was specified and the nonequilibrium extrapolation method[17] is applied.

3. Results and Discussion

Firstly, simulation in a straight circular tube is performed. The diameter is represented by 41 lattice nodes (40 δ_x) and the length of the tube is 20 times of the height. Here, we take the streamwise momentum accommodation coefficient $\sigma = 1$ as almost all engineering calculations.[3] The pressure distribution along the microtube predicted from the first slip boundary condition is[3]

$$\tilde{p}(\tilde{x}) = -8Kn_o + \sqrt{(8Kn_o)^2 + (1 + 16Kn_o)\tilde{x} + (Pr^2 + 16Kn_oPr)(1 - \tilde{x})}\,, \tag{6}$$

where $\tilde{p} = p(x, r)/p_o$, $\tilde{x} = x/L$, L is the tube length. Pr is the ratio of the inlet and outlet pressure.

The pressure drop along the tube which deviate from linear pressure drop for $Pr = 2$ with different outlet Knudsen number Kn_o are shown in Fig. 2. Comparing with the analytical solution Eq. (6), good results were obtained by LBM simulation. Figure 2 demonstrated that the larger Kn_o is, the smaller the deviation from the linear pressure distribution. It is also observed the rarefaction effect and the compressibility effect on the pressure distribution are contradictory.

In Fig. 3, the variation of slip velocity along the microtube wall is presented. The streamwise velocity profile (first-order slip-flow model) given by Weng *et al.*[3] can also be written as

$$U(x, r) = -\frac{D^2}{16\mu}\frac{dp}{dx}\left(1 - 4\left(\frac{r}{D}\right)^2 + \frac{4Kn_o}{\tilde{p}}\right)\,. \tag{7}$$

Hence, the analytical solution for slip velocity on the wall normalized by the central velocity at outlet U_{oc} is

$$\frac{U_{\text{slip}}(x)}{U_{\text{oc}}} = \frac{d\tilde{p}/d\tilde{x}}{(d\tilde{p}/d\tilde{x})_o}\frac{Kn}{(0.25 + Kn_o)}\,, \tag{8}$$

where $d\tilde{p}/d\tilde{x}$ is the nondimensional pressure gradient and the $(d\tilde{p}/d\tilde{x})_o$ means the pressure gradient at exit, which can be calculated by Eq. (6).

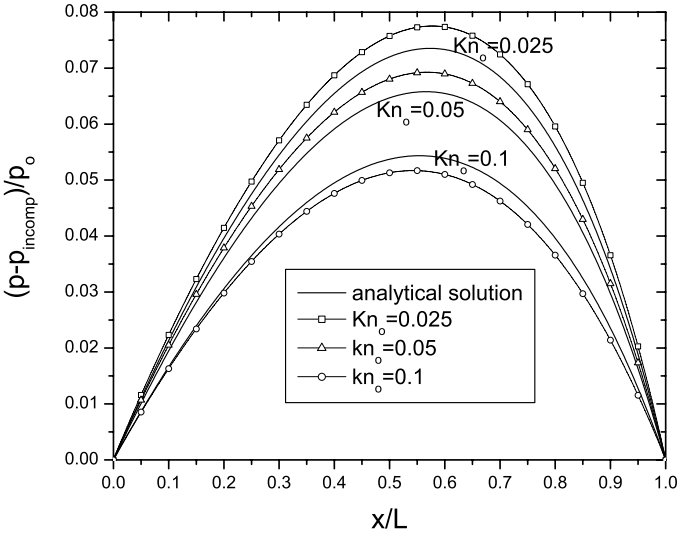

Fig. 2. Pressure distribution along the tube for different Kn_o ($Pr = 2$).

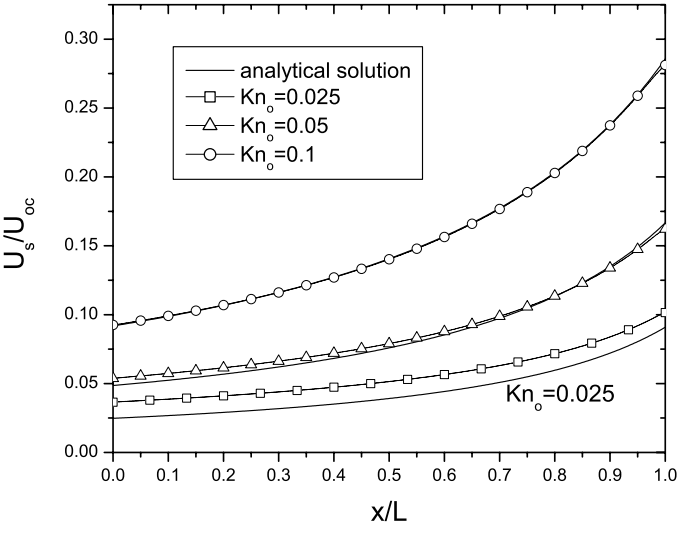

Fig. 3. Slip velocity in wall along the tube for different Kn_o ($Pr = 2$).

From Fig. 3, we can see that the slip velocity on the wall would increase with x. For cases of $Kn_o = 0.025$, 0.05, 0.1, the slip velocity on wall obtained by LBM agrees well with the analytical solution.

For the cases of microtube with sudden expansion or contraction, the geometry is illustrated in Fig. 1. In our simulations $L_i = L_o$ and the ratio of diameter of wide part and narrow part is 2. To simulate the axisymmetric flow, uniform lattices

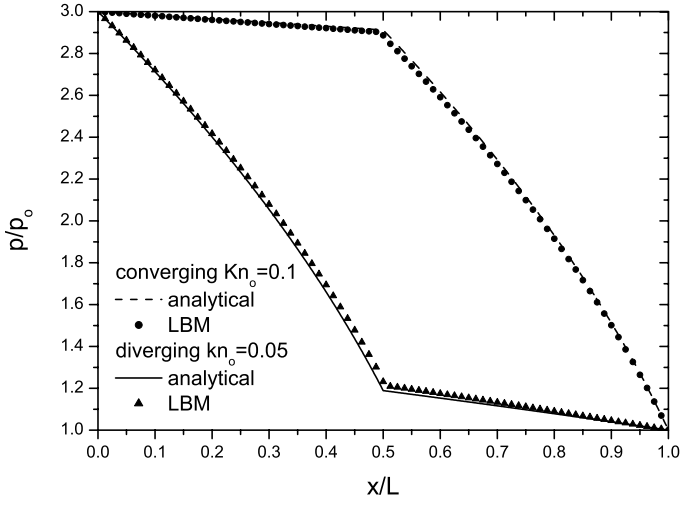

Fig. 4. Pressure distribution in converging and diverging tubes obtained by analysis and LBM.

are used. The narrow and wide parts are represented by 21 and 41 lattice nodes with diameter $20\delta_x$ and $40\delta_x$, respectively. In the streamwise direction, 401 lattices represent L_i and L_o.

For the two segments of the tubes, if the pressure at junction P_j is known, applying the Eq. (6) twice, we can obtain the pressure distribution along the whole microtube. P_j can be easily obtained through mass conservation in the two part of tube.[3,9] Here we did not consider the additional pressure loss term as Lee *et al.*[9] who attributed the measured pressure drop near junction to a loss during transition. In Fig. 4, the pressure distributions at the axis for $Pr = 3$ in the converging and diverging tubes are shown. The pressure variation is nonlinear and there is a discontinuity in slope at the junction which may be due to change of cross-sectional area and compressibility effect. Very small discrepancy between analytical and LBM solutions can be observed. It seems the gas flow in these tubes is still affected by the junction.

The distributions of slip wall velocity U_s in converging and diverging tubes obtained by analysis and LBM are illustrated in Fig. 5. Our numerical solutions agree well with the analytical results except the small discrepancy in the small region near the junction and the segment after the junction in diverging tube. It seems the gas slip flow is affected by the junction. In Fig. 5, we can see that there is a jump around the junction and U_s shows a negative value just before (converging case) or behind (diverging case) the junction. The negative value means there is a vortex in the corner. That would also be demonstrated clearly in Figs. 6 and 7.

Figure 6 gives out the streamlines for several cases with different Kn_o in diverging tubes. In Figs. 6 and 7, the dash-dot line represents the axis of microtubes. For the case $Kn_o = 0.01$, at the corner a big vortex appears. Lee *et al.*[9] had conjectured

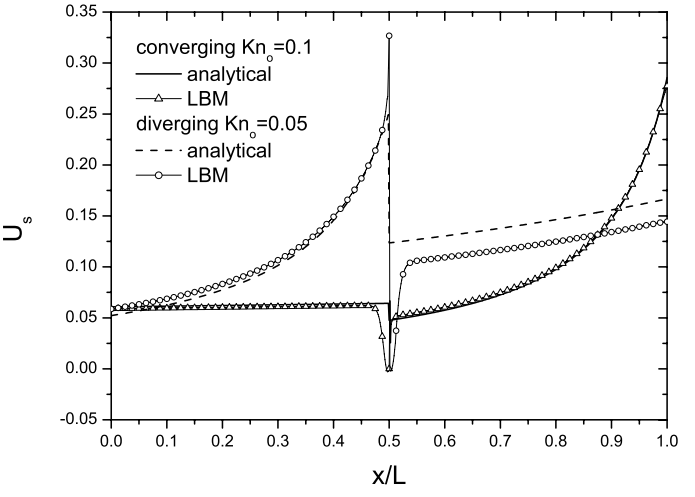

Fig. 5. Wall slip velocity distribution in converging and diverging tubes obtained by analysis and LBM, U_s is normalized by the central outlet velocity of each segment.

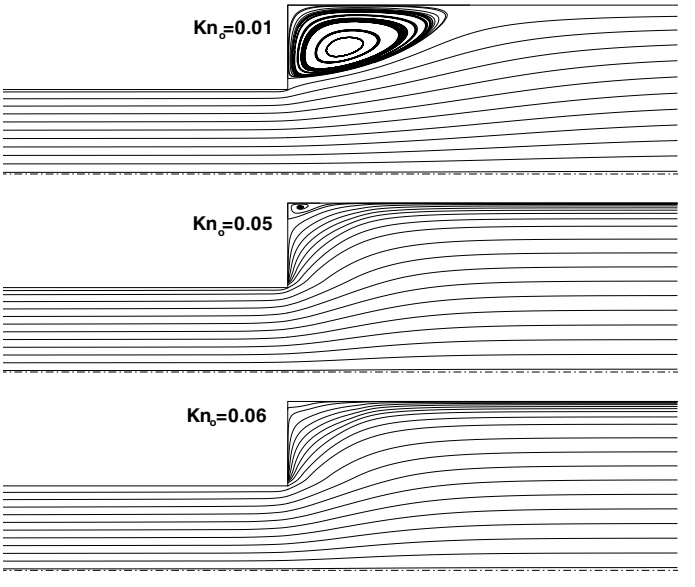

Fig. 6. Streamlines in microtubes with sudden expansion.

that there are secondary flows, such as vortices in the corner based on their experiments about constricted microchannel. Our numerical results confirmed that in cases of lower Kn_o. However, for the case of $Kn_o = 0.05$, the vortex strength at the corner would decrease and the vortex disappears in the case of $Kn_o = 0.06$. For cases of high Kn_o (i.e. $Kn_o > 0.06$), the flow in microtube with sudden expansion

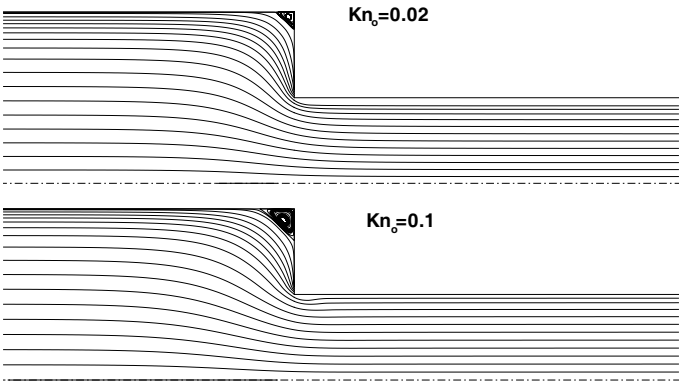

Fig. 7. Streamlines in microtubes with sudden contraction.

does not separate at the corners and the streamlines are attached to boundary. As we know, the formation of vortex is usually due to two factors: viscosity and sufficient velocity gradient. Existent of relatively large slip velocity at the wall would greatly reduce the velocity gradient. As a result, the vortex disappears in sudden expanded microtube when Kn_o is high.

Figure 7 gives out the streamlines for two cases with different Kn_o in converging tubes. For both cases, at the corner a very small vortex appears, which is consistent with deduction of Lee *et al.*[9] based on experiments. In the above cases, there is no *vena contracta* or the *vena contracta* is too small to detect.

4. Conclusions

In summary, with an axisymmetric lattice Boltzmann D2Q9 model, the gas slip flows in microtubes with a sudden expansion or contraction with $0.01 < Kn_o < 0.1$ are simulated. With the boundary condition combined specular and bounce-back schemes, the pressure and the slip velocity distributions along the microtube all agree well with the analytical results. A jump of slip velocity at wall near to the junction and vortex at corner all demonstrate the effect of the junction. For microflows of lower Kn_o (i.e. $Kn_o = 0.01$) in the sudden expanded tube, a vortex appears at the corner behind the junction. With higher Kn_o, the strength of the vortex would decrease or disappear (i.e. $Kn_o = 0.06$). For microflows in the sudden constricted tube, a very weak vortex appears at the corner just before the junction. The results are consistent with some experiment conclusions.

References

1. M. Gad-el-Hak, *J. Fluids Eng.* **121**, 5 (1999).
2. E. B. Arkilic, M. A. Schmidt and K. S. Breuer, *J. MEMS* **6**, 167 (1997).
3. C. I. Weng, W. L. Li and C. C. Hwang, *Nanotechnology* **10**, 373 (1999).
4. A. Beskok and G. Karniadakis, *AIAA* Paper 93-3269 (1993).

5. E. Piekos and K. Breuer, *AIAA* Paper 95-2089 (1995).
6. C. Y. Lim, C. Shu, X. D. Niu and Y. T. Chew, *Phys. Fluids* **14**, 2299 (2002).
7. G. H. Tang, W. Q. Tao and Y. L. He, *Int. J. Mod. Phys. C* **15**, 335 (2004).
8. A. Agrawal, L. Djenidi and R. A. Antonia, *J. Fluid Mech.* **530**, 135 (2005).
9. W. Y. Lee, M. Wong and Y. Zohar, *J. Fluid Mech.* **459**, 187 (2002).
10. I. Halliday, L. A. Hammond, C. M. Care, K. Good and A. Stevens, *Phys. Rev. E* **64**, 011208 (2001).
11. T. S. Lee, H. Huang and C. Shu, *Int. J. Numer. Meth. Fluids* **49**, 99 (2005).
12. H. Huang, T. S. Lee and C. Shu, *Int. J. Numer. Meth. Fluids* **53**, 1707 (2007).
13. Y. Peng, C. Shu, Y. T. Chew and J. Qiu, *J. Comput. Phys.* **186**, 295 (2003).
14. X. D. Niu, C. Shu and Y. T. Chew, *Int. J. Mod. Phys. C* **14**, 785 (2003).
15. Y. H. Qian, D. d'Humieres and P. Lallemand, *Europhys. Lett.* **17**, 479 (1992).
16. S. Succi, *Phys. Rev. Lett.* **89**, 064502 (2002).
17. Z. Guo, C. Zheng and B. Shi, *Chinese Phys.* **11**, 366 (2002).
18. G. H. Tang, W. Q. Tao and Y. L. He, *Int. J. Mod. Phys. C* **18**, 805 (2007).
19. H. Huang, T. S. Lee and C. Shu, *Int. J. Numer. Meth. Heat Fluid Flow* **17**, 587 (2007).